Experimental and Plant Data of Pneumatic Conveying Characteristics of Seven Granular Polyethylene Resins in Horizontal and Vertical Pipes

F. Pon, K.K. Botros, P. Grabinski, B. Quaiattini
NOVA Chemicals Research & Technology Centre
Calgary, Alberta, Canada

and

L. Motherwell
NOVA Chemicals Corporation, Joffre Site
Joffre, Alberta, Canada

Prepared for Presentation at the AIChE Annual Meeting, Particle Technology Forum, Pneumatic Conveying
November 7-12, 2004, Austin, Texas.

ABSTRACT

A pilot-scale conveying test facility was constructed to study the pneumatic conveying behaviour of various granular polyethylene resins in horizontal and vertical pipes. The facility is fully instrumented to measure air and solid flow rates, fluid temperature and pressure at various locations around the loop, and also allowed visual observation of the flow pattern in the pipe. Seven granular polyethylene resin grades, manufactured with two different catalyst systems, were tested and the corresponding impact and friction pressure drop coefficients were obtained for the horizontal and vertical sections of the loop. Comparisons between these coefficients reveal that some resins exhibit pressure loss coefficients that are double the values measured for other grades, and hence pose conveying limitations in a given system. This is despite their apparent similarity in their respective morphologies, bulk densities and other properties. The solid-to-air velocity slip ratio for all the grades was also determined. Somewhat surprisingly, its value was very similar across all grades. However, its behaviour as a function of airflow Froude number was consistent with literature data. Different degrees of wall fouling, as measured by monitoring the air-only pressure drop, were also observed for the different resins. Dimensionless state diagrams were developed from the experimental observation of saltation and minimum pressure points. These results compared favorably to data collected at a manufacturing facility for the seven resins tested.

NOMENCLATURE

A = pipe cross-sectional area
c = solid particle velocity
C_D = solid particle drag coefficient
C_{Df} = solid particle free falling drag coefficient
d = particle diameter
D = pipe internal diameter
f = Darcy friction factor

Fr = airflow Froude number defined as: $Fr = v/\sqrt{gD}$

Fr^* = solids-flow Froude number defined as: $Fr^* = c/\sqrt{gD}$

g = acceleration of gravity

G = solids mass flow rate

L = pipe length

ΔP_G = pressure drop due to gravity

ΔP_L = pressure drop due to air alone

ΔP_Z^* = pressure drop due to solids impact and friction

Q = air mass flow rate

R = conveying pipe bend radius (m)

Re = Reynolds number of mean air flow based on pipe diameter ($\rho vD/\eta$)

Re_p = Reynolds number based on particle relative velocity and particle diameter ($\rho vd/\eta$)

v = mean air flow velocity

w_f = solids settling velocity

Greek Letters:

α = inclination angle

β = gravity parameter

η = air dynamic viscosity

δ = constant

ε = pipe internal roughness

ρ = air density

ρ_p = solid particle density

ρ^* = apparent solids flow density

μ = solids loading ratio (G/Q)

λ_Z = pressure loss coefficient due to solids (including gravity)

λ_Z^* = solids impact and friction pressure loss coefficient

χ = constant

ψ = particle sphericity

1.0 INTRODUCTION

Pneumatic conveying is a very practical method for in-plant distribution of large amounts of dry powdered, granular, and pelletized materials. In dilute phase conveying [1], solid particles are introduced into a fast flowing gas stream (normally air) where solids remain suspended and separated from each other. Such process systems operate at relatively low pressure and consequently are comparatively inexpensive to install.

In the simplest of positive pressure systems, a blower generates an air stream in the conveying pipeline at a pressure up to about 1 bar-g. The material to be conveyed is fed in a controlled manner into this pipeline, and is carried by the airflow to a destination point where the air is vented and the solid is collected in a receiving bin. The plastics industry has used such systems to transport granular fluff and pellets for many years. Despite the fact that there is a vast literature on the pneumatic conveying of solids [1,2], data regarding the pneumatic

conveying characteristics of granular polyethylene (PE) is scarce, e.g. [3]. Generally, the conveying characteristics of any granular material is greatly dependent on its specific morphology, particle size distribution, particle density, sphericity, stickiness, and its attrition property in relation to the internal wall of the conveying line. No two granular PE resin grades are identical in so far as their conveyability characteristics, despite the apparent similarity in their properties. Additionally, conveying system vendors and consultants recognize that system design is rarely straightforward, so each has their own techniques for sizing PE conveying systems.

Polyethylene manufacturing plants are often required to push plant systems to their capability limits, including conveying systems. Conveying lines have been observed to function significantly differently with only apparent minor variations in resin properties. This invariably affects or compromises the capacity of the systems that convey granular reactor resins to other areas of the plant site, and in many situations bottlenecks the plant production. Simplified simulation models indicate that the air velocity is more than high enough to ensure stable system behaviour. However, in reality the systems often behave in an unstable and unpredictable manner with specific resin grades. What should be smooth and steady operation is instead characterized by intermittent pressure spikes, indicative of slugging flow. Plant production is compromised when these spikes shut down the conveying system.

Furthermore, hardware modifications could be necessary to ensure conveying systems are not a bottleneck. But while simple in principle, the gas-solid flow in a conveying line is extremely complex and highly dependent on the characteristics of the solids as mentioned earlier. From the feed point to the outlet, the superficial air velocity nearly doubles, increasing pressure drop and pipe erosion, and risking product degradation or plate-out on the pipe walls. The “obvious” solution of increasing blower capacity then becomes less obvious when these factors are taken into account. Changing pipe size or re-routing the pipes increases retrofit costs.

In order to ensure that the most economical retrofit design is used that can accommodate the full range of products and anticipated production rates, a better understanding of the fundamental properties of the specific solids being transported that influence conveyability is needed. This understanding would then be built into a simulation tool that would allow full assessment of the various design options before field modifications are implemented.

This paper describes a pilot-scale dilute-phase pneumatic conveying test facility at the NOVA Chemicals Research and Technology Centre. The main objective is to determine precisely the conveying characteristics of seven specific PE granular resins produced at NOVA Chemicals’ manufacturing facilities. A theoretical framework is constructed to analyze the results obtained in the pilot-scale facility so that these results could be applied to commercial-scale facilities. Differences in the conveyability of these resins in terms of their respective friction and impact pressure loss coefficients, flowability, and characteristics are highlighted. Comparison with plant data from a manufacturing site is provided where applicable.

2.0 PILOT-SCALE FACILITY AND TEST PROCEDURE

The test facility consists of a 40 HP centrifugal compressor driven by a variable speed electric motor that supplies filtered air to a piping loop. The loop is composed of two horizontal sections from the feed point followed by a vertical section before discharging into a receiving bin, as shown in Fig. 1. All sections are constructed from 0.1 m ID aluminum pipe interconnected by long radius (R/D = 9.6) elbows. The overall length of the test loop from the feed point to the receiving bin is approximately 30 m. Axial length of each individual connecting spool is given in Fig. 1. Granular polyethylene resins are fed from a 1 m^3 capacity feed bin into the flowing air stream through a variable speed rotary valve. A receiving bin is located directly above the feed bin to allow dumping of the resins into the feed bin via a connecting gate valve (not shown). The receiving bin is mounted on independent frames on four weigh cells in order to facilitate solid mass flow measurements during the test. Therefore, flexible hoses are used to connect the receiving end of the conveying loop as well as the filtered outlet air duct so as not to affect solid mass flow measurement.

Temperature and pressure measurements (indicated by letters T and P, respectively in Fig. 1) are taken along the three straight sections of pipe (two horizontal, and one vertical as shown in Fig. 1). Airflow rate is measured via an annubar located upstream of the polyethylene feed point. All measurements are recorded by a high-speed data acquisition system for later processing. Measurement uncertainties are as follows: airflow rate 1% of range, temperature $\pm$ 0.1°C, static pressure 0.2% of range, differential pressure 0.1% of range.

The test protocol is as follows. First, targets for air velocity and solids-to-air mass ratio are set. The airflow set point is established on the blower and the air pressure, temperature and flow rate are measured at the blower discharge. The polyethylene solids are then metered into the air stream by the rotary valve. Absolute and differential pressures are measured for the various straight sections (i.e. static P1, P2 and P3, and differentials between P1-P2, P3-P4, and P5-P6, locations of which are shown in Fig. 1). The weight of the receiver bin is also continuously measured to verify the solids flow rate. One run represents a full discharge of the feed bin (~1 m^3 of resin) and receipt of the same in the receiving bin, before the gate valve between the two is opened to recycle the resin for the next run. The solids-free (i.e., air-alone) pressure drop of the loop was observed to change during some test campaigns. To account for this, the air-only pressure drop was measured every 5 runs.

Seven grades of granular polyethylene were selected for testing. These grades are a subset of the types manufactured at NOVA Chemicals' plants, and were selected on the basis of spanning the range of conveying performance at the plants, and the measured physical properties of the materials. These grades are listed in Table 1.

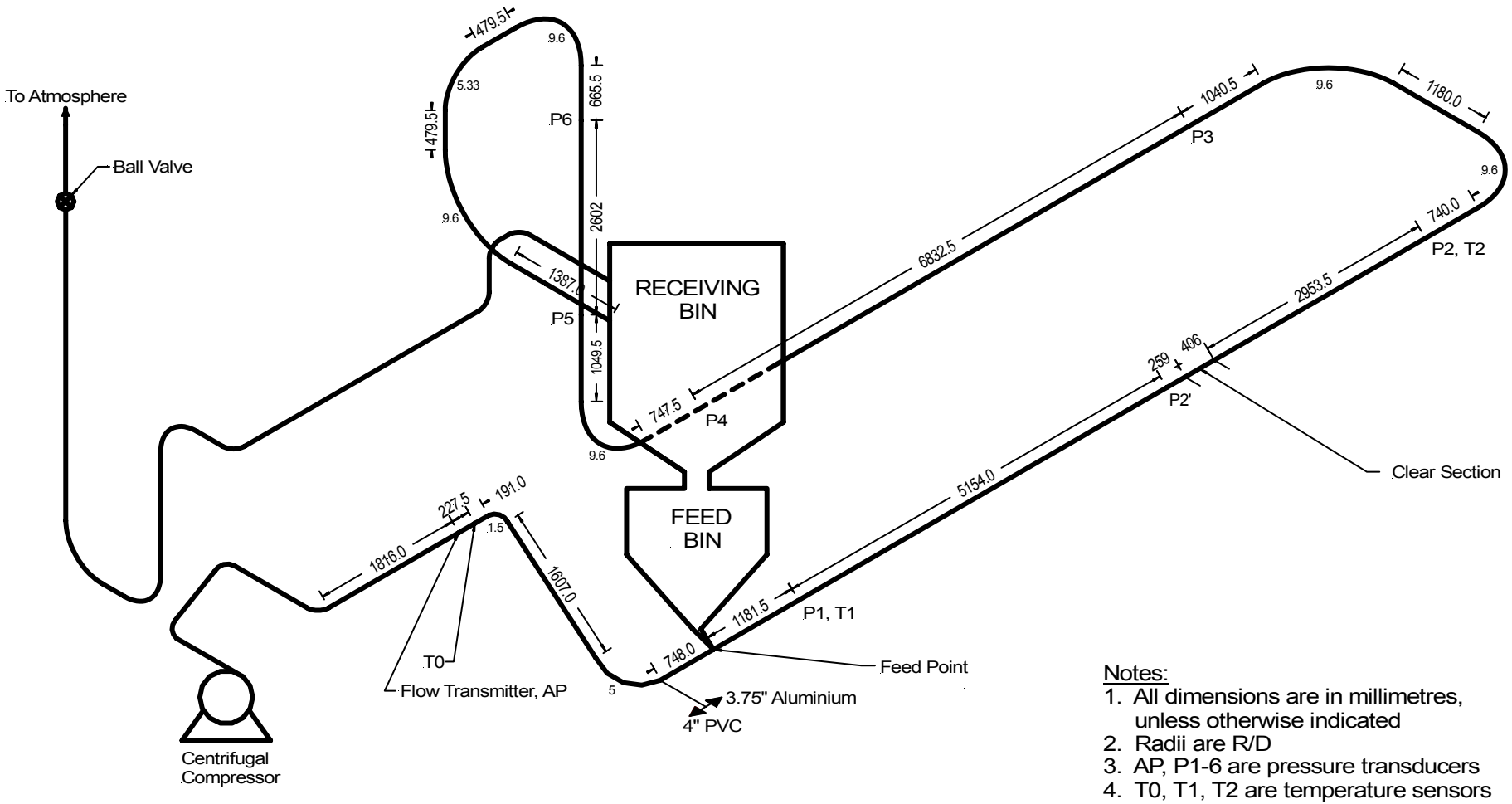

Figure 1: Pneumatic conveying test loop at NOVA Chemicals Research & Technology Centre.

Table 1: Grades of Polyethylene Tested.

Grade	Melt Index* (g/10 min)	Density** (g/cm^3)	Comonomer Type	Catalyst Type
A	20	0.924	1	2
B	1	0.918	2	1
C	1	0.918	1	1
D	0.8	0.916	2	1
E	3	0.938	2	1
F	7	0.935	2	1
G	20	0.924	1	1

* Melt Index: $I_{2.16}$, ASTM D1238 condition 190/2.16
** Density: ASTM D792

3.0 GOVERNING EQUATIONS

The conveyability characteristics of the various granular polyethylene resins are assessed by means of the following commonly used parameters:

a) solid impact and friction pressure loss coefficient, λ^*_z;
b) state diagram defining the saltation limit or boundary between dense and dilute phases of the conveying system; and
c) slip ratio, defined as the ratio of the particle velocity to the air velocity, *c/v*.

The first parameter defines the demand requirement on the air blower in terms of delivery pressure and flow rates. The second parameter determines a balancing act between the mean airflow velocity and pipe diameter, while the final parameter *c/v* determines how well the solid particles flow with the carrier fluid. The following are the fundamental formulations of these parameters.

The overall pressure drop along a constant area pipe with air-conveyed solid particles can be written as [1,2]:

$$\Delta P = \Delta P_L + \Delta P^*_z + \Delta P_G \tag{1}$$

The first term, ΔP_L, is attributed to the contribution to the pressure drop from the airflow alone, which can be determined from:

$$\Delta P_L = f\left(\frac{1}{2}\rho v^2\right)\frac{L}{D} \tag{2}$$

where *f* is the 'Darcy' friction factor which is function of Reynolds number of the mean flow based on pipe internal diameter, D, and the relative roughness of the pipe, which can be determined from a derivative of Colebrook-White equation in the following explicit form [4]:

$$f = \frac{0.25}{\left[\log\left(\frac{\varepsilon}{3.7D} + \frac{5.74}{\mathrm{Re}^{0.9}}\right)\right]^2} \tag{3}$$

The air mean flow velocity, v, is determined from: $Q = \rho\, v\, A$. The second term in eq. (1), ΔP_Z^* describes the pressure drop due to solid impact and friction which can be expressed in terms of (λ^*_z) as follows:

$$\Delta P^*_z = \lambda^*_z \left(\frac{1}{2}\rho^* c^2\right)\frac{L}{D} \tag{4}$$

where ρ^* is the solid apparent bulk (or superficial) density determined from: $G = \rho^*\, c\, A$. The last term in eq. (1) describes the contribution of gravity to the overall pressure drop. Weber [5] derived a general fundamental expression for the gravity contribution as follows:

$$\Delta P_G = \mu \left(\frac{2\beta}{\left(\frac{c}{v}\right)Fr^2}\right)\left(\frac{1}{2}\rho\, v^2\right)\frac{L}{D} \tag{5}$$

where, β, is a gravity term expresses in terms of the pipe inclination, α, (positive if sloped upward along the flow direction), and the settling velocity (w_f), as follows:

$$\beta = \sin(\alpha) + \frac{w_f}{v}\cos^2(\alpha) \tag{6}$$

where

$$w_f = \sqrt{\left[\frac{C_D}{C_{Df}}(v-c)^2\,\frac{2c/v}{\lambda_z Fr^{*2}}\right]} \tag{7}$$

$$\lambda_z = \lambda^*_Z\left(\frac{c}{v}\right) + \frac{2\beta}{\left(\frac{c}{v}\right)Fr^2} \tag{8}$$

The above equations can be solved iteratively to determine both λ^*_z and c/v utilizing the following auxiliary relationships for settling velocity of spherical particles, effects of sphericity (ψ) and the drag coefficient (C_D):

$$W_f = \left[\frac{4\,d\left(\rho_p - \rho\right)}{3\,C_D\,\rho}\,g\right]^{1/2} \tag{9}$$

$$\left(W_f\right)_\psi \;/\left(W_f\right) = 0.843\log_{10}\left(\psi / 0.065\right) \tag{10}$$

$$C_D = \frac{24}{\mathrm{Re}_P} + \frac{4}{\sqrt{\mathrm{Re}_P}} + 0.4 \tag{11}$$

In order to compare conveyability in terms of the saltation limit from the experimental facility to observations from the same resin grades in a manufacturing plant, a generalized dimensionless state diagram was used. Fig. 2 shows a representative diagram and the three dimensionless numbers defined as follows:

- Solids loading in terms of the dimensionless parameter μ,
- Airflow Froude number, *Fr*, and
- The dimensionless constant parameter, $G/(\rho\, A\sqrt{g\,D})$.

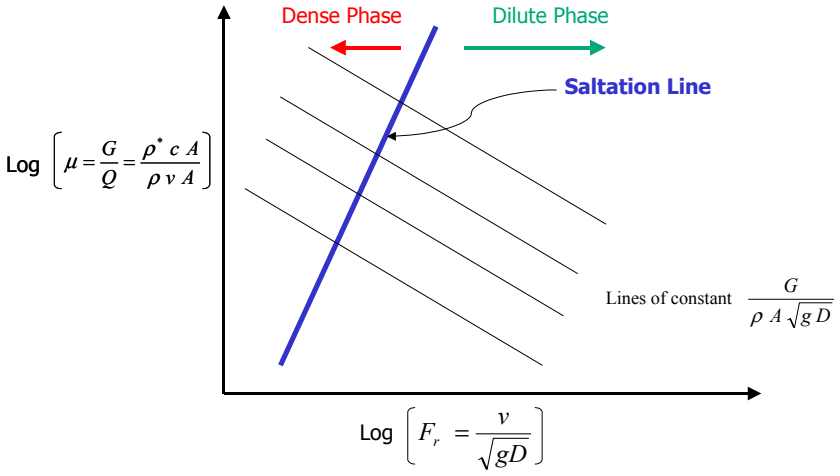

Figure 2: Definition of Dimensionless State Diagram Parameters.

This leads to the commonly used expression of the saltation line [1], which is also referred to as the "P_{min} line" as follows:

$$\mu = \frac{1}{10^{\delta}} Fr^{\chi} \tag{12}$$

where, δ and χ are two characteristics constants to be determined by fitting experimental data of the saltation point at different solids loadings and Froude numbers.

4.0 RESULTS

4.1 Air-Only Friction

During a test campaign of a given resin (i.e., a series of runs or cycles of the same resin grade through the loop), the pressure drop along the loop with air-alone flow was observed not to be repeatable under identical test conditions. In order to accurately determine the pressure drops due to solids, the variation in the air-alone contribution to the overall pressure drop must be properly accounted for according to eq. (1). This was achieved by conducting air-alone tests after every five runs (or cycles) with resin.

Fig. 3 shows an example of the effect of the changes in the experimentally determined air-alone Darcy friction coefficient for a particular PE resin (grade E) during one campaign of a total of 35 runs (cycles). For this particular resin grade, the resin tested in the campaign prior to this one had coated the pipe wall, resulting in a high friction coefficient at the start of the experiment (0 cycles). After 5 cycles, the friction coefficient decreased, likely due to a scrubbing effect of the pipe wall resin layer. As the experiment progressed, the friction coefficient was observed to increase or decrease randomly. All other six PE grades exhibited

similar behavior, and these variations in the air-alone pressure drop were taken into account in the determination of the solids impact and friction pressure drop (as in eq. 1). It is worth noting that the friction coefficient is shown to be increasing with Re in the range of Re > 100,000 unlike the trend exhibited in the well-known Moody diagram. This is likely due to the wall coating by PE resins, which is consistent with Nikuradse's measurements with epoxy and sand coating [6].

These changes in the air-alone friction coefficient were likely caused by the resin altering the characteristics of the pipe wall surface roughness. During the course of specific solid conveying runs, the polyethylene resins changed the surface characteristics of the wall by continuously depositing or removing a thin film of polymer on the wall. This action was evidently random, and therefore the variation in the air-alone friction coefficient was not only different for each resin grade but also varied from run to run within a test campaign of the same grade.

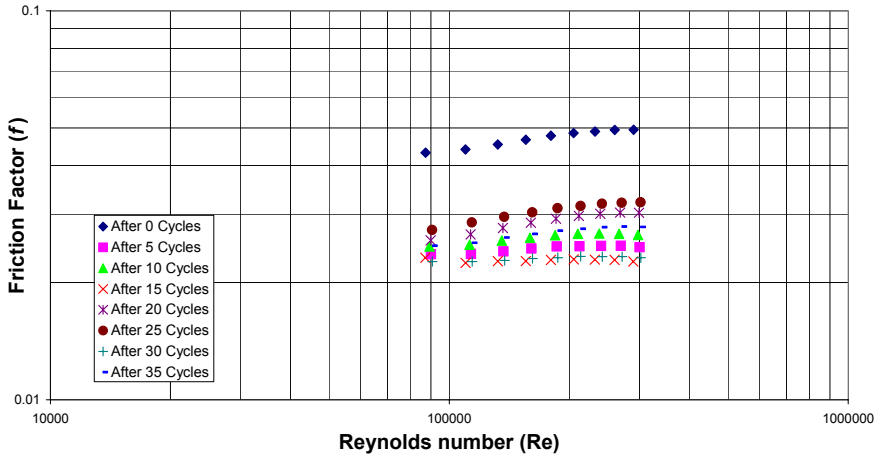

Figure 3: Air-Alone Experimentally Determined Darcy Friction Factor (Polyethylene Grade E).

An attempt was made to characterize the type of surface coating deposited on the pipe walls. A sample of the film was peeled off the pipe wall and its thickness measured with a thickness gauge. The thickness was found to be too thin (around 0.5 mm) to have been a significant effect on reducing the cross sectional area of the pipe. (Note that the friction coefficient is proportional to D^5, hence a 1 mm reduction in the pipe I.D. of 0.1 m results in only a 5% increase in the friction coefficient). The sample was also photographed on edge with a Scanning Electron Microscope (SEM) as shown in Fig. 4. It shows that the surface roughness is clearly visible, from which an average roughness was estimated to be around 250 microns, rather high compared to the roughness of new aluminum pipe, which was in the order of only 5-10 microns. This explains the apparent relatively high air-alone friction coefficient determined experimentally. In fact, when a roughness value of 250 microns is introduced in eq. (3) along with the range of Reynolds number in the present tests and D = 0.1 m, the calculated friction coefficient is in the same range as those determined experimentally in Fig. 3.

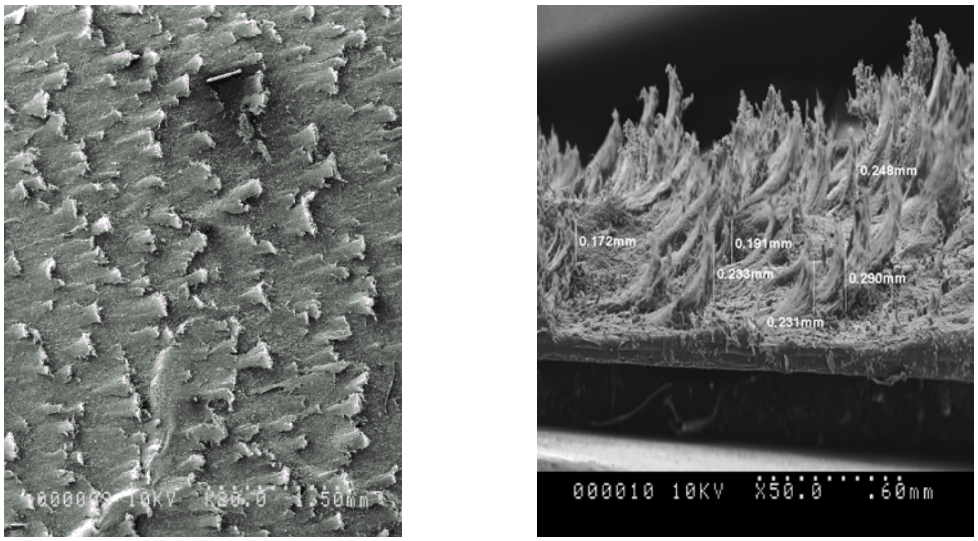

Figure 4: SEM Photomicrograph of Typical Pipe Coating after Several Runs (Plan View and a Cut-Through View).

4.2 Solids Impact and Friction

The second term in eq. (1) is related to the contribution to the pressure drop due to solids impact and friction, ΔP^*_z, which is described by the coefficient λ_Z^* in eq. (4). Sample results of this coefficient for grade E as a function of Froude number, Fr, for different solids loadings in the horizontal and vertical sections are shown in Figs. 5 and 6, respectively. The air-alone pressure drop, ΔP_L in eq. (1), is determined using eq. (2) in which the Darcy friction factor, *f*, is updated every five test cycles. This updating improves the repeatability of λ_Z^* calculated using eq. (1). A more precise determination of λ_Z^* could have been obtained with an air-alone test performed between each solid test cycle. However, error analysis of the air-alone tests indicates that, for the variation in *f* shown in Fig. 3 being approximately 0.01, the resulting error bar on λ_Z^* is ±0.006 at Fr = 25 and ±0.001 at Fr = 45. Additionally, the third term in eq. (1) has to first be calculated from eq. (5) and then deducted from the overall pressure drop in the respective horizontal or vertical section.

As seen in Fig. 5, λ_Z^* decreases as the Froude number increases, and reaches asymptotes at Froude numbers between 20 and 25. Additionally, it appears that the solids loading μ has a minor effect on the asymptotic value of λ_Z^*. This behavior is consistent with data in literature (e.g., for Styropor material [2]) and could be attributed to the characteristics of dilute phase behaviour in this range of Fr. Detailed analysis involving particle mechanics would be helpful in providing some insight into the physics of this behaviour. The high λ_Z^* observed at low Fr (Fr<20) in the vertical section is indicative of the erratic system behaviour caused by saltation. This is perhaps due to the fact that the transition into dense phase conveying in a vertical section is characterized by the gravity force directly opposing the solids flow momentum force, unlike the case in a horizontal section.

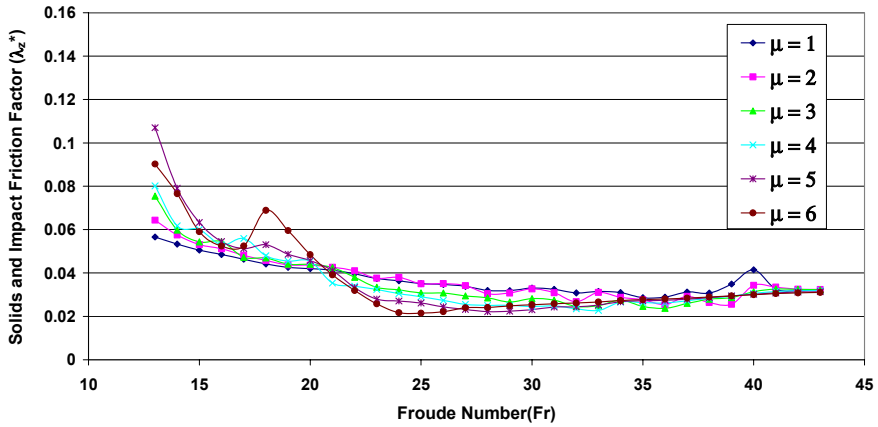

Figure 5: Solids Impact and Friction Factor (λ_Z^*) for a Horizontal Section of Pipe (Polyethylene Grade E).

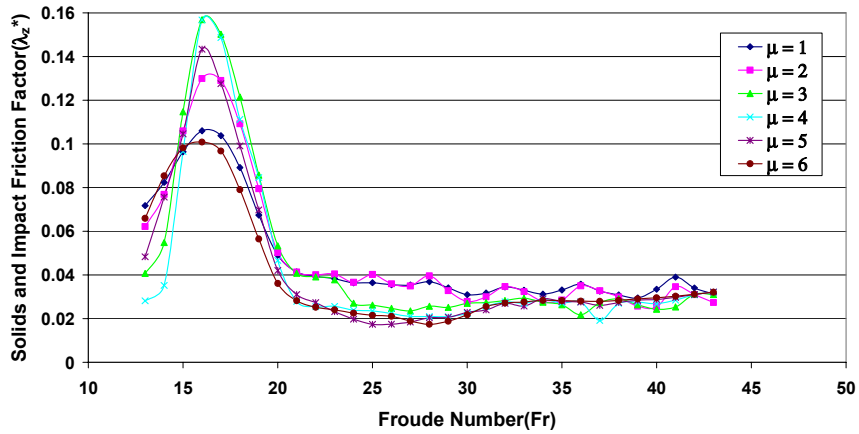

Figure 6: Solids Impact and Friction Factor (λ_Z^*) for a Vertical Section of Pipe (Polyethylene Grade E).

Table 2 compares experimentally determined solids impact and friction factors (λ_Z^*) for all seven PE resin grades tested, at the asymptotic range of Froude number. Based on these values, grade G is shown to have the highest λ_Z^* value while grade A has the lowest, in a horizontal section. In a vertical section, grade G still has the highest value, with grade B having the lowest. It is interesting to note that λ_Z^* for grade A in both horizontal and vertical sections is lower than grade G, even though they have the same polymer characteristics and resin morphology. The only difference is that grade A has lower hexane extractables, and exhibits lower stickiness characteristics than grade G. Grade A is also produced with a different (new) catalyst than grade G. In fact, it has been observed [7] that PE products made using this new catalyst consistently display improved flowability and conveyability characteristics. Finally, except for grade B resin, λ_Z^* appears to be consistently higher in the vertical section than in the horizontal section. This observation was also true in the case of Styropor [2].

Table 2: Experimentally Determined Solids Impact and Friction Factor (λ_Z^*) at $F_r > 25$.

Resin Grade	Horizontal Section	Measurement Variation (1σ) Horizontal	Vertical Section	Measurement Variation (1σ) Vertical
A	0.021	0.0040	0.052	0.0066
B	0.022	0.0020	0.020	0.0038
C	0.022	0.0013	0.033	0.0039
D	0.023	0.0023	0.034	0.0031
E	0.029	0.0038	0.031	0.0035
F	0.032	0.0030	0.049	0.0049
G	0.040	0.0025	0.070	0.0070

4.3 Slip Ratio

As previously mentioned, the slip ratio (c/v) is a measure of the "flowability", or "floatability", of the solid particles with respect to the carrier air stream. Obviously, a higher slip ratio is indicative of better flowing characteristics of the resin in the transporting medium, since the resin approaches the velocity of the air. Results for the grade E resin are shown in Figs. 7 & 8 for different solids flow rates in the horizontal and vertical sections, respectively. Table 3 shows the asymptotic values of the slip ratio for all seven grades. These values are between 0.72 and 0.83 in the horizontal section and between 0.65 and 0.76 in the vertical section. Grades A, D, and E have the highest slip ratios, whereas grade C has the lowest. The data show that, in the range of solids flow rates considered, the slip ratio characteristics with respect to air flow velocity are the same. This indicates that the slip ratio is dependent more on the particle morphology and sphericity, as well as pipe orientation, than on solids flow rates.

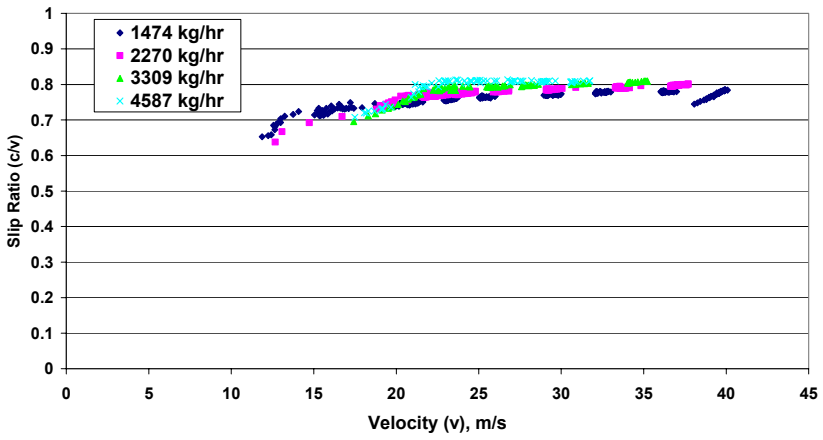

Figure 7: Slip Ratio in the Horizontal Section (Polyethylene Grade E).

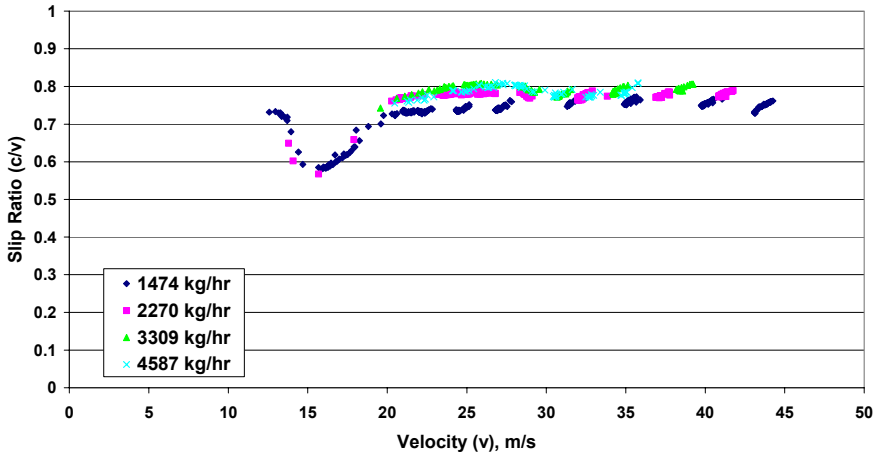

Figure 8: Slip Ratio in the Vertical Section (Polyethylene Grade E).

Table 3: Maximum Slip Ratio.

Resin Grade	Horizontal Section	Measurement Variation (1σ) Horizontal	Vertical Section	Measurement Variation (1σ) Vertical
A	0.83	0.05	0.76	0.04
B	0.79	0.03	0.73	0.03
C	0.72	0.03	0.65	0.02
D	0.80	0.02	0.76	0.02
E	0.79	0.04	0.77	0.03
F	0.80	0.04	0.73	0.04
G	0.79	0.04	0.73	0.05

4.4 State Diagram:

For each resin grade, a dimensionless state diagram as defined in Fig. 2 has been constructed based on the experimental data obtained from the pilot-scale facility. The minimum pressure point at each solids loading was determined from visual observation of the flow pattern (i.e. onset of saltation) through the clear spool section located in the middle of the first horizontal section (see Fig. 1). The minimum pressure (P_{min}) line was then obtained by fitting the minimum pressure points using eq. (12), and the values for the constants δ and χ was thus obtained. An example of the dimensionless state diagram for PE resin grade E is shown in Figs. 9 and 10 for the horizontal and vertical sections, respectively.

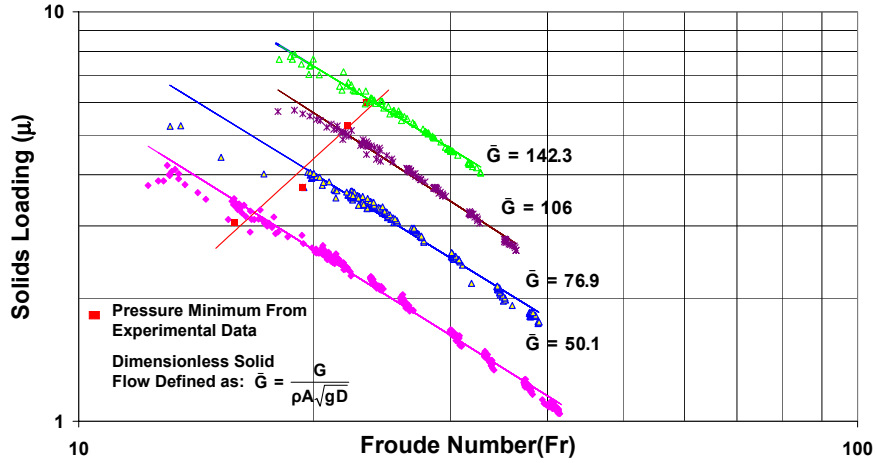

Figure 9: Dimensionless State Diagram for the Horizontal Section (Polyethylene Grade E).

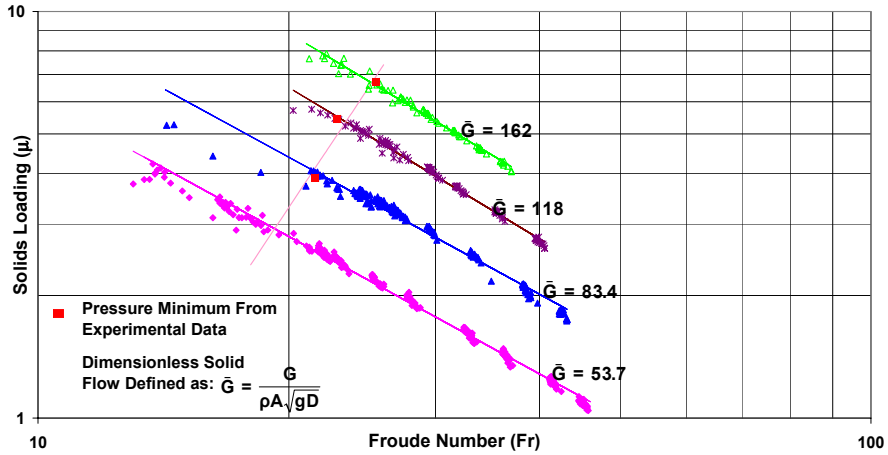

Figure 10: Dimensionless State Diagram for the Vertical Section (Polyethylene Grade E).

Figures 11 and 12 show a comparison of the fitted P_{min} lines for all seven resin grades tested for the horizontal and vertical sections, respectively. It appears that the P_{min} lines for some grades exhibit different slopes on the log-log scale of the state diagram than others. Note that since the slope of the P_{min} line is indicative of the minimum Fr at saltation for a given solids flow, the steeper the slope the lower the minimum air velocity required for dilute conveying operation. A similar notion can be also inferred by the shift caused by the parameter δ. Table 4 lists the constants δ and χ for these P_{min} lines for both the horizontal and vertical sections. These are important results that can be used to determine the minimum Froude number (hence velocity for a given line size) for a stable operation of the system. For example, if a solids loading μ of 4.0 is required, the minimum velocity in a 0.3 m diameter horizontal pipe section should be greater than 39.5, 41.0, 36.4, 33.9, 32.6, 36.9 and 35.6 m/s for grades A, B, C, D, E, F and G, respectively. These minimum velocities can be calculated for a different line size or solid loadings, hence exemplifying the value of these dimensionless state diagrams.

Table 4: Experimentally Determined Constants δ and χ for the P_{min} Lines.

	Horizontal		Vertical	
Resin Grade	δ	χ	δ	χ
A	1.575	1.598	4.002	3.216
B	0.8653	1.064	4.135	3.234
C	3.657	3.211	4.239	3.394
D	3.851	3.437	3.490	3.081
E	1.624	1.741	4.837	3.808
F	3.608	3.159	2.261	2.014
G	2.863	2.631	14.34	10.65

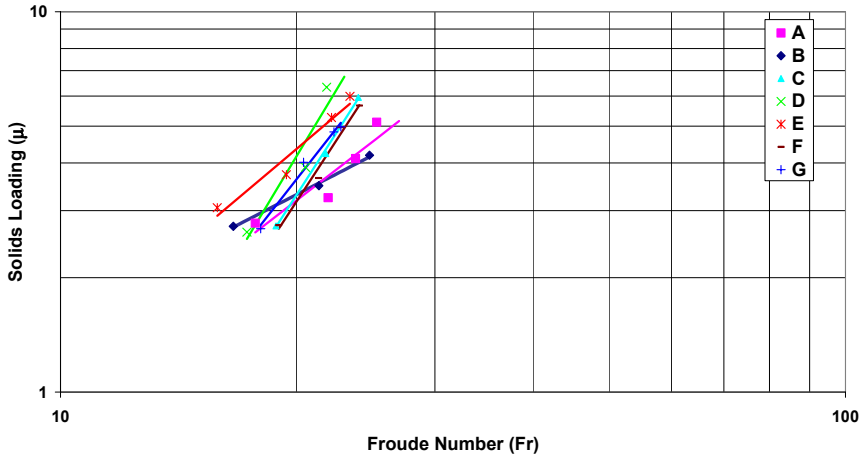

Figure 11: P_{min} for all Resin Grades for the Horizontal Section.

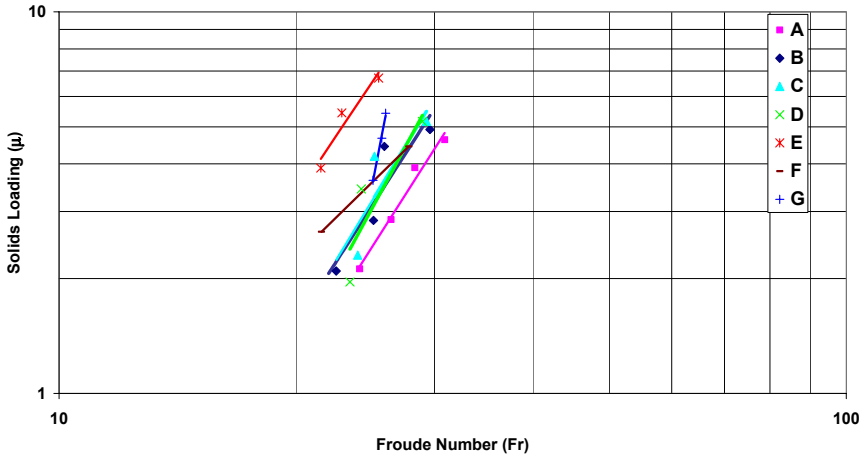

Figure 12: P_{min} for all Resin Grades for the Vertical Section.

All horizontal data obtained from the pilot-scale facility for the seven grades were pooled on one state diagram and all P_{min} lines were reduced to an average line as shown in

Fig. 13. Plant measurements were also taken on different conveying sections of different line sizes and a total length of approximately 300 m. These data were normalized and plotted on the dimensionless state diagram of the pooled data from the pilot facility as shown in Fig. 13. With its positive displacement constant speed blower, the plant system is constrained to operate at a single Froude number value of approximately 20. It appears, therefore, that the plant conveying system is limited to a solids loading μ of 3.5 due to this constraint on the maximum air flow.

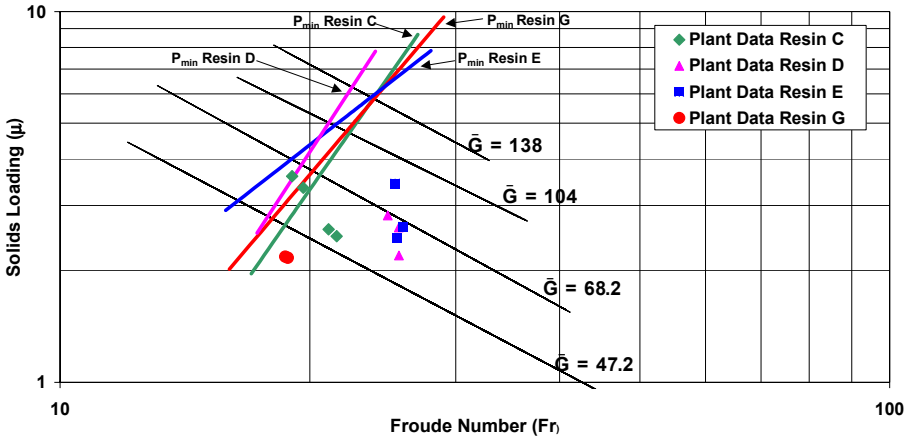

Figure 13: Horizontal Dimensionless State Diagram - Plant Performance vs. Pilot-Scale Facility Data.

4.5 Particle Size and Morphology

The average particle size of resins tested in the pilot-scale facility is shown in Table 5. Each resin was tested every 5-10 cycles to assess attrition. No measurable decrease in average particle size was observed. The differences in particle morphology of four of the grades tested are shown in Fig. 13. Notice that the particle morphology of grades B and C are similar, as are grades A and G. Recall that grade G resin exhibited the highest λ_Z^* values among the seven grades tested, while grades A, B, and C exhibited the lowest (see Table 2). This leads to the conclusion that there is no strong correlation between the particle size or morphology with solids impact and friction factor. Further examination of the morphology of other grades substantiated this observation.

Table 5: Particle Size Analysis of Laboratory Tested Resins.

Resin Grade	Average Particle Size* (mm)
A	0.558
B	0.743
C	0.950
D	0.664
E	0.614
F	0.63
G	0.567

* Particle Size Sieve Analysis: ASTM D1921

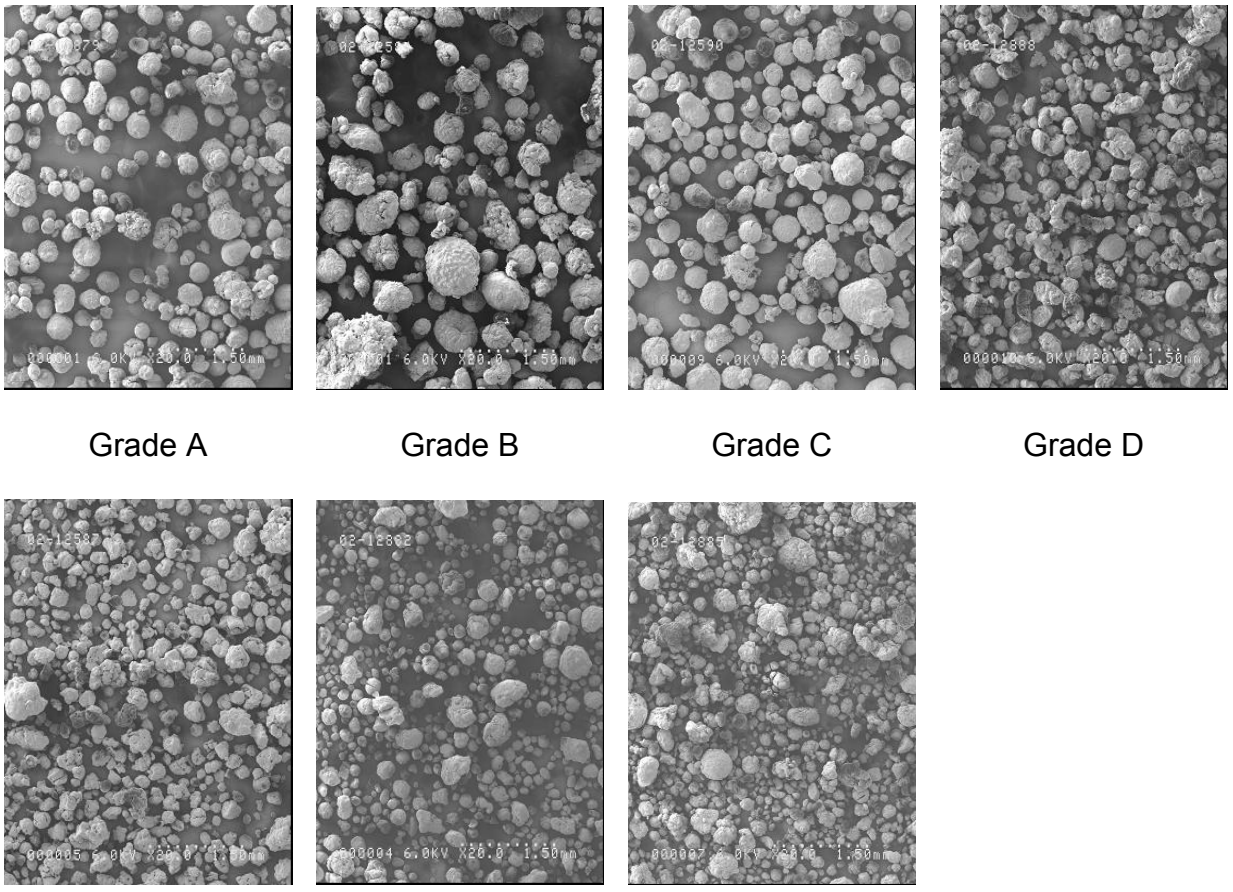

Grade A Grade B Grade C Grade D

Grade E Grade F Grade G

Figure 14: SEM Photomicrographs of the Polyethylene Resin Grades Tested.

5.0 CONCLUSION

A pilot-scale test facility was used to assess the conveyability of seven granular polyethylene resin grades. These grades showed different behavior in so far as the solids impact and friction pressure loss coefficients and saltation limits, but not slip ratios.

It was shown that generally, the solids impact and friction pressure loss coefficient, λ_Z^*, decreases as the Froude number, Fr, increases, and reaches asymptotes at $20 \leq Fr \leq 25$. The solids loading ratio, μ, appears to have minor effects on the asymptotic value of λ_Z^*, and an insight into this observation warrants some further investigation. Detailed analysis involving particle mechanics would be helpful in providing some insight into the physics of this behaviour and perhaps quantify the contribution from particle-particle interaction to the overall value of λ_Z^*. Additionally, it was observed that λ_Z^* is consistently higher in the vertical section than in the horizontal section.

It appears that the P_{min} lines for some resin grades differ primarily in their respective slopes on a log-log scale of the dimensionless state diagram. These lines were used to assess conveyability limitations in an actual PE manufacturing facility. With its positive displacement constant speed blower, the plant system was found to be constrained to operate at a single value of $Fr \cong 20$, hence it is limited in so far as its maximum solids loading ratio, μ.

Finally, differences in particle morphologies or average particle sizes between the seven grades do not appear to have a strong correlation with λ_Z^*.

6.0 ACKNOWLEDGMENTS

The authors would like to thank Michael James, Tyler Dubetz, Steve Cooke and Roger Mason for regular operation of the test facility, and Dr. Benjamin Shaw for his thorough review of the manuscript. We also thank NOVA Chemicals Corporation for granting permission to publish this work.

7.0 REFERENCES

1. Zenz, F.A. and Othmar, D.F., *Fluidization and Fluid Particle Systems*, Reinhold, New York, 1962.
2. Marcus, R.D., Leung, L.S., Klinzing, G.E. and Rizk, F., *Pneumatic Conveying of Solids*, Chapman and Hall, London, 1990.
3. Li, H. and Tomita, Y.: "An Experimental Study of Swirling Flow Pneumatic Conveying System in a Vertical Pipeline", ASME Journal of Fluids Engineering, vol. **120**, pp.200-202, March 1998.
4. Miller, D.S., *Internal Flow Systems*, 2nd Edition, Chapter 8, Gulf Publishing Company, 1990.
5. Weber, M., *Strömungs Fördertechnik*, Mainz, Krausskopf, 1974.
6. Schlichting, H., *Boundary Layer Theory*, McGraw-Hill Inc., N.Y., p. 617, 1979.
7. Ker, V., Unpublished data, NOVA Chemicals Corporation, Calgary, Alberta, Canada, 2001.